ELSEVIER

Biochimica et Biophysica Acta 1371 (1998) 363–370

BIOCHIMICA ET BIOPHYSICA ACTA
BBA

Characterization of swollen lamellar phase of dimyristoylphosphatidylcholine–gramicidin A mixed membranes by DSC, SAXS, and densimetry

Yukihiro Kobayashi, Kazuhiro Fukada *

Department of Chemistry, Faculty of Science, Tokyo Metropolitan University, Minamioosawa 1-1, Hachiohji, Tokyo 192-0397, Japan

Received 24 November 1997; revised 3 March 1998; accepted 11 March 1998

Abstract

For the fully hydrated multilamellar stack of dimyristoylphosphatidylcholine (DMPC) fluid membranes containing hydrophobic peptide gramicidin A (GrA), the membrane thickness and the bilayer–bilayer separation (i.e., water layer thickness) were determined by measuring small-angle X-ray scattering and the density of aqueous suspensions of DMPC–GrA mixtures. When the molar ratio of GrA to DMPC was 0.04, the membrane thickness decreased by 2–3 Å by the incorporation of GrA molecules into DMPC bilayers, whereas the water layer thickness increased by 3–4 Å. As the cause of the increment of water layer thickness, two possibilities were considered; (1) attractive van der Waals force acting between the bilayer membranes weakened by the decrease of membrane thickness, and (2) repulsive undulation force enhanced by the incorporation of GrA which may stabilize the gauche conformers of the lipid acyl chains.

Keywords: Phospholipid; Gramicidin A; Multilamellar phase; Bilayer–bilayer separation; Small-angle X-ray scattering; Densimetry

1. Introduction

Multilamellar structures of lipid bilayer membranes in excess water are good model systems for the study of forces acting between two large parallel plates. There are four main types of forces acting between lipid bilayers, commonly considered to be important: van der Waals, electrostatic, hydration, and undulation forces [1]. In the multilamellar systems, these forces compete with each other, and net attractive and repulsive forces determine the bilayer–bilayer separation, i.e., water layer thickness. These forces may vary with the composition of the medium, the lipid bilayer material itself, and incorporation of solute molecules into the lipid bilayers [2]. In this study, we focused attention to the effects of incorporation of a hydrophobic peptide, gramicidin A, into the electrically neutral phospholipid bilayers in aid of understanding the balance of above mentioned attractive and repulsive forces.

Abbreviations: DMPC, dimyristoylphosphatidylcholine; GrA, gramicidin A; SAXS, small-angle X-ray scattering; DSC, differential scanning calorimetry

* Corresponding author. Fax: +81-426-772525; E-mail: fukada-kazuhiro@c.metro-u.ac.jp

0005-2736/98/$19.00
PII S0005-2736(98)00043-1

Gramicidin A (GrA) is a linear polypeptide antibiotic that forms specific channels in lipid membranes for the transport of monovalent cations [3]. The amino acid sequence of GrA is as follows:

$$\overset{1}{\text{HCO-L-Val}}\text{-}\overset{2}{\text{Gly}}\text{-L-}\overset{3}{\text{Ala}}\text{-D-}\overset{4}{\text{Leu}}\text{-L-}\overset{5}{\text{Ala}}\text{-D-}\overset{6}{\text{Val}}\text{-L-}\overset{7}{\text{Val}}$$

$$\text{-D-}\overset{8}{\text{Val}}\text{-L-}\overset{9}{\text{Trp}}\text{-D-}\overset{10}{\text{Leu}}\text{-L-}\overset{11}{\text{Trp}}\text{-D-}\overset{12}{\text{Leu}}\text{-L-}\overset{13}{\text{Trp}}$$

$$\text{-D-}\overset{14}{\text{Leu}}\text{-L-}\overset{15}{\text{Trp}}\text{-NHCH}_2\text{CH}_2\text{OH},$$

and natural GrA contains 10% of isoleucine at the position 1 [4]. As shown in the above chemical structure of GrA, the carboxyl and amino termini are blocked with a formyl group and ethanolamine, respectively. Hence, this peptide has no electric charge. Also, we used a zwitterionic, electrically neutral phospholipid, dimyristoylphosphatidylcholine (DMPC), and therefore, the long range electrostatic repulsive force can be neglected.

In the present study, the phase behaviors of fully hydrated DMPC–GrA mixed systems were characterized. Further, the bilayer repeat distance and the bilayer–bilayer separation were determined by measuring small-angle X-ray scattering (SAXS) and the density of the DMPC–GrA suspensions.

2. Materials and methods

2.1. Sample preparation

1,2-Dimyristoyl-*sn*-glycero-3-phosphocholine (DMPC) was purchased from Avanti polar lipids (Birmingham, AL). It was confirmed from thermogravimetry that the lot we used contained two hydrated water molecules per DMPC molecule. The purity of the lipid was checked by thin-layer chromatography (TLC). Although two spots, one of which is a faint spot probably caused by lysolecithin, was detected on TLC, the data on DSC [5], SAXS [6–11], and densimetry [12–14] were in good agreement with the literature; so, we used this sample without further purification. Gramicidin A (GrA) was purchased from Fluka Chemie and used without further purification. Water was purified with Milli-Q labo (Millipore, Bedford, MA).

The hydrated DMPC–GrA mixtures were prepared as follows. Prescribed amounts of DMPC and GrA in required proportion were weighed and dissolved together in chloroform. The molar ratio of GrA to DMPC, R, was varied from 0 to 0.10. (R was calculated based on the following molecular weights; DMPC dihydrate = 713.97 and GrA = 1883.7). The solvent was evaporated under a stream of nitrogen gas, and then the sample was kept under vacuum for 3 h to remove remaining traces of solvent. The DMPC–GrA dry mixture was swelled by adding water containing 15 μM sodium azide as an antiseptic. The hydrated sample was annealed by more than five cycles of cooling at 0°C and heating at 50°C, and was aged overnight at room temperature. All GrA molecules in the samples can be solubilized in lipid membranes when R is below 0.1 [15], and the dissolution of GrA in water is negligible since solubility of GrA is extremely low (< 1 $\mu g/cm^3$) [16].

For the density measurements, we prepared aqueous suspensions of DMPC–GrA mixtures. The fully hydrated samples were vortex-mixed and gently sonicated for 15 min by a bath sonicator to prevent sedimentation of large multilamellar vesicles.

2.2. Differential scanning calorimetry

Differential scanning calorimetry (DSC) was performed using DSC220C (Seiko Instruments, Tokyo) at a heating rate of 0.25°C/min. The lipid content in the samples ranged from 20 to 30 wt.% where DMPC–GrA mixtures were fully hydrated.

2.3. Small-angle X-ray scattering measurement

Small angle X-ray scattering (SAXS) was measured by a high-resolution small angle X-ray scattering instrument equipped with a tungsten/silicon multilayer monochromator and a self-rotating anode system [17]. Monochromatic CuKα radiation ($\lambda = 0.154$ nm) from a rotating anode (SRAMXP18, Mac Science, Tokyo) operated at 40 kV and 350 mA was focused by the Kratky slit and introduced to the sample. The diffracted X-rays were detected by the digital imaging plate (DIP200, Mac Science). The length from the sample to the imaging-plate was about 109 cm. The temperature of samples, which were mounted to a 1 mm thick, Mylar-film-window

cell, was regulated to ± 0.1°C by the thermostat cell holder. The contents of water in the samples ranged from 30 to 90 wt.%. The lamellar repeat distance, D, was calculated from the peak position of the diffracted X-rays using the Bragg equation; $2D\sin\theta = n\lambda$ where n is integer and 2θ is scattering angle.

2.4. Density measurement

Density of aqueous suspensions of DMPC–GrA mixture was measured by using a digital density meter (DMA60/602, Anton Paar, Graz). Temperature of the sample cell was controlled by a thermostated water circulator (DC5/K20, Haake, Karlsruhe) and monitored by a digital thermometer with a platinum resistance probe (F250, Automatic systems lab., Bradville, Milton Keynes, UK). The scatter of temperature was ± 0.01°C. The accuracy of the density measurement was confirmed to be $\pm 5 \times 10^{-6}$ g cm^{-3}.

3. Results and discussion

3.1. Characterization of fully hydrated DMPC–GrA mixtures by DSC and SAXS

DSC heating thermograms of the fully hydrated DMPC–GrA mixtures are shown in Fig. 1. For the DMPC–water two-component system, two endothermic peaks were observed at 12°C and 23°C which correspond to pre- and main transitions, respectively. These transition temperatures and the estimated enthalpies agree well with the literature values [5]. When GrA was added to the system, these endothermic peaks broadened and the transition temperatures decreased with increasing GrA content. When the molar ratio of GrA to DMPC, R, exceeded 0.03, however, we could not detect the pretransition. These observations may be explained by the effect of GrA molecules incorporated in the lipid bilayers which perturb the alkyl-chain confinement of lipids and decrease the cooperativity of the phase transitions [15]. Similar results have been reported for the lipid–melittin mixtures where the pretransition disappears by incorporating melittin, a linear polypeptide with high affinity with lipid membranes [18,19].

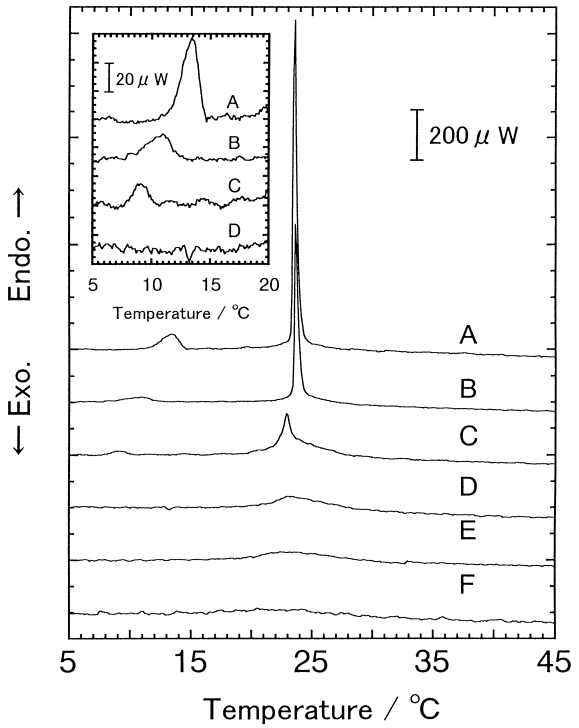

Fig. 1. DSC thermograms of fully hydrated DMPC–GrA mixtures (20–30 wt.% suspension), in which mole ratio of GrA to DMPC are 0 (A), 0.01 (B), 0.02 (C), 0.03 (D), 0.05 (E), and 0.08 (F). Heating rate is 0.25°C/min. The inset shows the DSC thermograms with which vertical is magnified.

Fig. 2 shows the representative small-angle X-ray diffraction patterns for the fully hydrated DMPC–GrA mixtures at 20°C and 37°C. For the DMPC–water two-component system at 20°C, the hydrated lipid is $P_{\beta'}$ and the Bragg reflections from (11) and (21) planes of periodically rippled structure were observed [6] as well as the first (10) and second (20) reflections from the multilamellar structure. Contrary to this, the reflections from the rippled structure were not observed for the samples containing GrA. It is thought that the ripple periodicity of DMPC was disrupted by the incorporation of GrA. At 37°C where the lipid is in the liquid crystalline state, two peaks corresponding to the first and second reflections from the lamellar stack of fluid bilayers were observed for the samples with the composition of $0 \leq R \leq 0.10$.

From the peak position of diffracted X-rays, the lamellar repeat distance, D, was calculated and plotted against temperature in Fig. 3a. Above the main transition temperature of fully hydrated DMPC–GrA

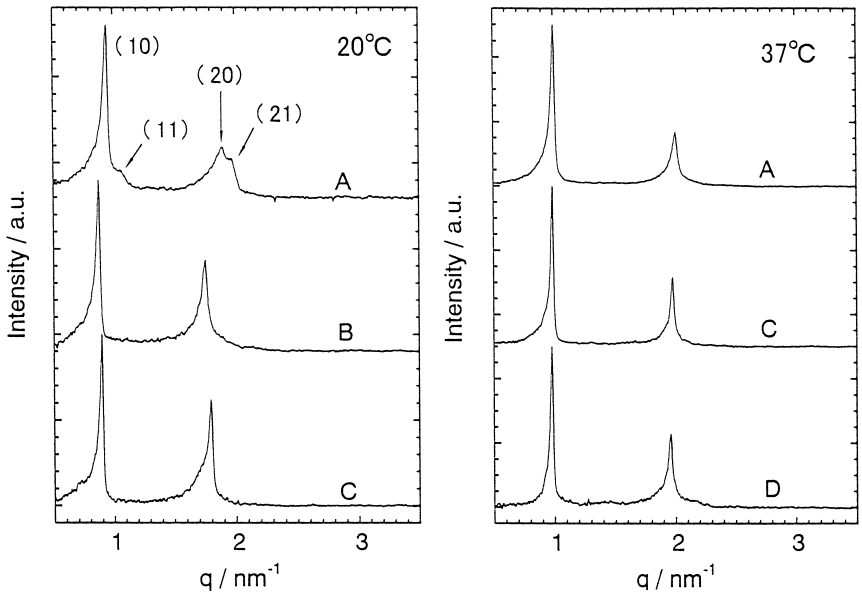

Fig. 2. Representative small angle X-ray diffraction patterns for fully hydrated DMPC–GrA mixtures at 20°C and 37°C. Molar ratios of GrA to DMPC are 0 (A), 0.005 (B), 0.04 (C), and 0.08 (D). q is magnitude of scattering vector: $q = 4\pi \sin\theta/\lambda$, where 2θ is scattering angle and λ is a wavelength of the X-ray. For the fully hydrated DMPC (sample A), four peaks are observed at 20°C, and assigned as (10), (11), (20), (21) in accordance with Ref. [6].

mixture ($\gtrsim$ 23°C), the lamellar repeat distance for the samples with $0 \leq R \leq 0.08$ decreased with increasing temperature up to 35°C and then leveled off in the temperature region from 35°C to 50°C [7–9]. When $R = 0.10$, the lamellar repeat distance has a minimum around 33°C, and then increased with increasing temperature above 33°C. In Fig. 3b, the lamellar repeat distances are replotted as a function of GrA content. At 20°C where the lipid is in gel state, the lamellar repeat distance had a maximum (72.2 Å) around $R = 0.005$ and it gradually decreased with GrA content when R exceeded 0.005. At the temperatures above the main transition (34 or 37°C), on the other hand, the monotonous increase in lamellar repeat distance with the GrA content was confirmed. Although we are interested in the behaviors of lipid membranes both below and above the main transition temperature, we focused the investigation on the liquid crystalline state in the present study.

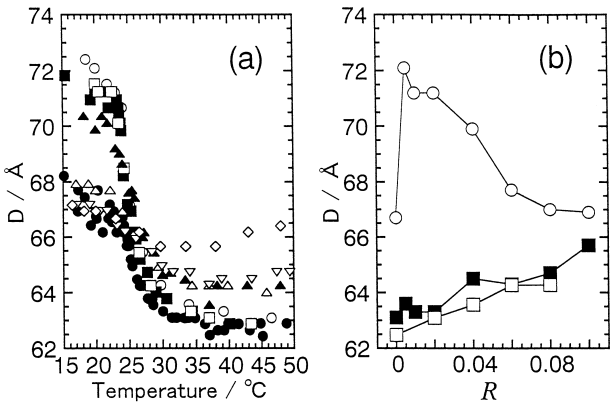

Fig. 3. (a) Lamellar repeat distance fully hydrated DMPC–GrA mixtures, D, plotted against temperature. Molar ratios of GrA to DMPC are 0 (●), 0.005 (○), 0.01 (■), 0.02 (□), 0.04 (▲), 0.06 (△), 0.08 (▽), and 0.1 (◇). (b)Lamellar repeat distance of the fully hydrated DMPC–GrA mixtures plotted against molar ratio of GrA to DMPC, R at 20°C (○), 34°C (■), and 37°C (□), respectively.

3.2. Limiting water content in DMPC–GrA–water systems

To determine the limiting water content in the fully hydrated multilamellar phase in excess water, the lamellar repeat distance was measured as a function of the water content (see Fig. 4). In the low water content region where the sample is not fully

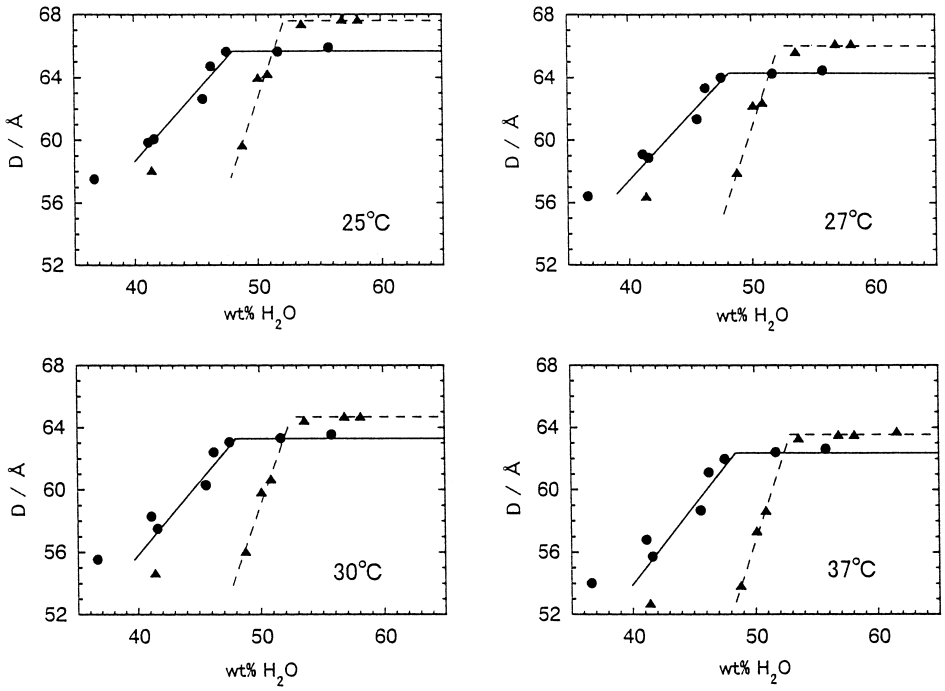

Fig. 4. Lamellar repeat distance of the multilamellar phase, D, as a function of water content. Molar ratio of GrA to DMPC are 0 (●) and 0.04 (▲).

hydrated, the lamellar repeat distance linearly increases with the water content. Above the limiting water content composition where the two-phase coexistence (multilamellar phase + bulk water) is observed, the repeat distance levels off. So, the limiting water contents can be determined from the break points in Fig. 4.

In the case of DMPC–water two-component system ($R = 0$), the limiting water content was ca. 48 wt.% and almost independent of the temperature ranging from 25 to 37°C. For the DMPC–GrA–water three component system ($R = 0.04$), on the other hand, the limiting water content was 52 wt.% at 25°C which gradually increased up to 53 wt.% with the temperature rise up to 37°C. The limiting water content of stacked DMPC bilayers in the liquid crystalline state increased by 4–5 wt.% by the incorporation of GrA. This result may suggest that the water layer thickness (i.e., bilayer–bilayer separation) in multilamellar phase increases by the incorporation of GrA. To evaluate the water layer thickness for these systems, the specific volume of DMPC–GrA mixed membranes was measured by densimetry as below.

3.3. Specific volumes of DMPC–GrA mixtures in L_α phase

By measuring the density of the aqueous suspension of DMPC–GrA mixtures, the apparent volume of the DMPC–GrA mixed membranes, Φ_v, was calculated by using the following equation:

$$\Phi_v = \frac{1}{c\rho} - \frac{1-c}{c} v_w^0 \quad (1)$$

where ρ is the density of the suspension, c is the weight fraction of the DMPC–GrA mixture in the suspension, and v_w^0 the specific volume of pure water. In Fig. 5a, Φ_v of DMPC–GrA mixtures in excess water is plotted against the molar ratio of GrA to DMPC. We can see that the apparent specific volume of the DMPC–GrA mixture monotonously decreases with increasing GrA content.

Here, we introduce the apparent volume of the mixture containing 1 g DMPC, V_1, which is expressed as

$$V_1 = \Phi_v(1 + R_w) \cong v_{DMPC} + R_w v_{GrA} \quad (2)$$

where v_{DMPC} and v_{GrA} are the specific volumes of

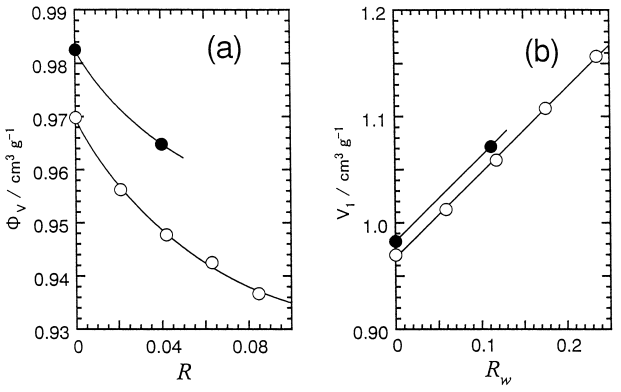

Fig. 5. (a) Apparent specific volume, Φ_v, of DMPC–GrA mixtures in excess water plotted against molar ratio of GrA to DMPC, R, at 25°C (○) and 37°C (●). (b) Apparent volume of the mixtures containing 1 g DMPC, V_1, plotted against weight ratio of GrA to DMPC, R_w, at 25°C (○) and 37°C (●). From the slope of the straight line, the volume of gramicidin A molecule is estimated to be 2.50 nm^3.

DMPC and GrA in bilayer membranes, respectively, and R_w the weight ratio of GrA to DMPC. In Fig. 5b, V_1 is plotted against R_w, where the slope corresponds to the specific volume of GrA (see Eq. (2)). The least-squares fitting was applied to the data points in Fig. 5b, which gives $v_{GrA} = 0.800$ cm^3 g^{-1} ($= 2.50$ nm^3 molecule^{-1}). This value agrees with the molecular model of GrA helical dimer with 1.5 nm diameter and 2.5–3.0 nm height in lipid-bilayer membranes [3]. This may be regarded as one of the evidences confirming that the GrA molecules in the system are entirely incorporated in the lipid-bilayer in the composition range studied here.

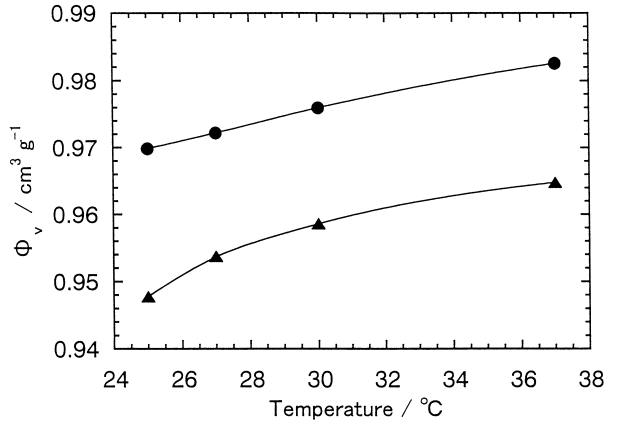

Fig. 6. Temperature dependence of apparent specific volume, Φ_v, of DMPC–GrA mixtures in excess water. Molar ratios of GrA to DMPC are 0 (●) and 0.04 (▲).

Fig. 6 shows the temperature dependence of Φ_v for the DMPC suspension with $R = 0$ and 0.04. The Φ_v value increased with increasing temperature, indicating that the occupied area per DMPC molecule in bilayers increased with the temperature rise.

3.4. Estimation of the bilayer–bilayer separation

By combining the above-mentioned SAXS and densimetry data, the water layer thickness in the multilamellar phase, D_w, can be calculated as follows. When one assumes that the ratio of the bilayer thickness, D_l, to the lamellar repeat distance, D, is equal to the volume fraction of the membranes in the multilamellar phase, ϕ, one can obtain following equation:

$$D_w = D - D_l = (1 - \phi)D. \quad (3)$$

On the other hand, ϕ is expressed as

$$\phi = \left\{1 + \frac{(1 - c^L)\bar{v}_w^L}{c^L \bar{v}_l^L}\right\}^{-1} \quad (4)$$

where c^L is the weight fraction of DMPC–GrA mixture in the multilamellar phase, $\bar{v}_l^L$ and $\bar{v}_w^L$ are the partial specific volumes of the mixture and of water in the multilamellar phase, respectively. In excess water condition, $1 - c^L$ is equal to the limiting water content of the system, which were already estimated in Fig. 4. By assuming $\bar{v}_l^L \cong \Phi_v$ and $\bar{v}_w^L \cong v_w^0$, one can calculate D_w and D_l in DMPC–GrA–water systems from Eqs. (3) and (4).

The above procedure is called a Luzzati method. It has been pointed out that the Luzzati method involves systematic errors because the defect regions in the multilamellar contain a disproportionate amount of water which do not contribute to the lamellar repeat distance [20]. In the case of DMPC–water system, however it has been reported that D_w estimated by the Luzzati method and that obtained from the electron density profile analysis is very similar [8]. So, the systematic error in this study may be negligibly small.

Fig. 7 shows the lamellar repeat distance (D), corresponding membrane thickness (D_l), and the wa-

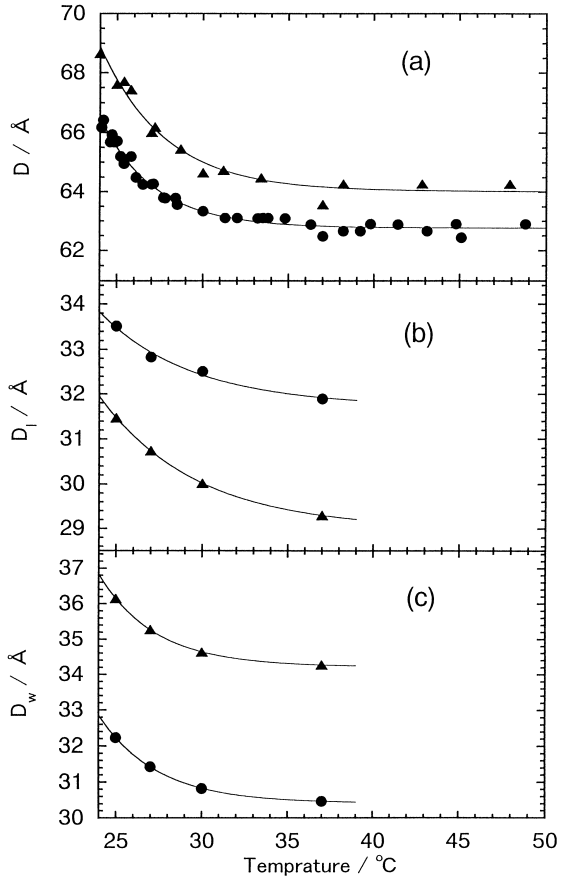

Fig. 7. Lamellar repeat distance, D, membrane thickness, D_l, and water layer thickness, D_w, of the fully hydrated multilamellar phase as a function of temperature. Molar ratio of GrA to DMPC are 0 (●) and 0.04 (▲).

ter layer thickness (D_w) for the fully hydrated DMPC and the DMPC–GrA mixtures with $R = 0.04$ as a function of temperature. For both the DMPC–water and DMPC–GrA water systems, the bilayer and the water layer thicknesses gradually decreased with increasing temperature. It is clearly seen that while the membrane thickness decreased by 2–3 Å by the incorporation of GrA into DMPC bilayer, the water layer thickness increased by 3–4 Å. Since the length of GrA helical dimer (2.5–3.0 nm) is smaller than the thickness of DMPC bilayer (3.2–3.4 nm), one can consider that the DMPC membrane is thinned by the incorporation of GrA to correct the mismatch of the length [3,21,22]. Also, it has been shown by FTIR measurements that the incorporation of gramicidin into lipid bilayers stabilizes gauche conformers of the lipid acyl chains in the liquid crystalline phase [16,23–26]. Since it is expected that the increase of gauche conformers in acyl chains leads to the decrease of bilayer thickness, our result indicating the decrease of membrane thickness by GrA incorporation is consistent with the FTIR studies.

As the cause for the increase of bilayer–bilayer separation by the GrA incorporation, we can consider the following two possibilities: (1) the decrease of attractive van der Waals force, and (2) the increase of repulsive undulation force. (Note that the net charge of DMPC molecule is zero and GrA molecule has no charge; therefore, the long range electrostatic repulsion between the membranes would be negligible. Also, the hydration force plays only a minor role at the separation of ca. 30 Å [27].) The attractive van der Waals force between two membranes in multilamellar phase, F_{vdW}, is expressed as

$$F_{vdW} = -\frac{H}{6\pi}\left\{\frac{1}{D_w^3} - \frac{2}{(D_w + D_l)^3} + \frac{1}{(D_w + 2D_l)^3}\right\} \quad (5)$$

where H is the Hamaker constant [28]. As the membrane thickness (D_l) decreases, one can expect from this equation that the van der Waals force acting between membranes will weaken and the bilayer–bilayer separation will increase. Besides this, one should consider the repulsive undulation force associated with the thermal fluctuations of the membranes. The undulation force between membranes derived by Helfrich, F_{undu}, is expressed as,

$$F_{undu} = \frac{3\pi(kT)^2}{64\kappa D_w^3} \quad (6)$$

where κ is the bending elasticity of membrane [29]. By the incorporation of GrA into bilayers, one may expect that the bending elasticity of membranes decreases because of the increase of gauche conformers in the lipid molecules, and the undulation force will increase. To fully clarify the role of incorporated GrA to the undulation force between membranes, however, further studies will be necessary where the bending rigidity of the membranes should be determined, e.g., by the micropipet manipulation technique [30].

Acknowledgements

This work was supported by the Fund for Specially Encouraged Research Project at Tokyo Metropolitan University to K.F.

References

[1] J.N. Israelachvili, Intermolecular and Surface Forces, 2nd edn., Academic Press, New York, 1991, p. 395.
[2] T. Hønger, K. Mortensen, J.H. Ipsen, J. Lemmich, R. Bauer, O.G. Mouritsen, Anomalous swelling of multilamellar lipid bilayers in the transition region by renormalization of curvature elasticity, Phys. Rev. Lett. 74 (1994) 3911–3914.
[3] B.A. Wallace, Gramicidin channels and pores, Annu. Rev. Biophys. Chem. 19 (1990) 127–157.
[4] E. Gross, B. Witkop, Gramicidin: IX. Preparation of Gramicidin A B, and C, Biochemistry 4 (1965) 2495–2501.
[5] D. Marsh, CRC Handbook of Lipid Bilayers, II.7, Calorimetric Data, CRC Press, Boca Raton, FL, 1990, p. 136.
[6] S. Matuoka, S. Kato, M. Akiyama, Y. Amemiya, I. Hatta, Temperature dependence of the ripple structure in dimyristoylphosphatidylcholine studied by synchrotron X-ray small-angle diffraction, Biochim. Biophys. Acta 1028 (1990) 103–109.
[7] R. Zhang, W. Sun, S. Tristram-Nagle, R.L. Headrick, R.M. Suter, J.F. Nagle, Critical fluctuations in membranes, Phys. Rev. Lett. 74 (1995) 2832–2835.
[8] S. Kirchner, G. Cevc, Temperature variation of lipid membrane structure and the hydration force in fluid lamellar phase: experimental studies with dimyristoylphosphatidylcholine multibilayers, Europhys. Lett. 23 (3) (1993) 229–235.
[9] J. Lemmich, K. Mortensen, J.H. Ipsen, T. Hønger, R. Bauer, O.G. Mouritsen, Pseudocritical behavior and unbinding of phospolipid bilayers, Phys. Rev. Lett. 75 (1995) 3958–3961.
[10] L.J. Lis, M. MacAlister, N. Fuller, R.P. Rand, V.A. Parsegian, Interactions between neutral phospholipid bilayer membranes, Biophys. J. 37 (1982) 657–665.
[11] M.J. Janiak, D.M. Small, G.G. Shipley, Temperature and compositional dependence of the structure of hydrated dimyristoyl lecithin, J. Biol. Chem. 254 (1979) 6068–6078.
[12] N.L. Gershfeld, Equilibrium studies of lecithin–cholesterol interactions: I. Stoichiometry of lecithin–cholesterol complexes in bulk systems, Biophys. J. 22 (1978) 469–488.
[13] J.F. Nagle, D.A. Wilkinson, Lecithin bilayers. Density measurements and molecular interactions, Biophys. J. 23 (1978) 159–175.
[14] R. Koynova, A. Koumanov, B. Tenchov, Metastable ripple gel phase in saturated phosphatidylcholines: calorimetric and densitometric characterization, Biochim. Biophys. Acta 1285 (1996) 101–108.
[15] M. Bouchard, M. Auger, Solvent history dependence of gramicidin–lipid interactions: a Raman and infrared spectroscopic study, Biophys. J. 65 (1993) 2484–2492.
[16] G. Kemp, K.A. Jacobson, C.E. Wenner, Solution and interfacial properties of gramicidin pertinent to its effect on membranes, Biochim. Biophys. Acta 255 (1972) 493–501.
[17] H. Yoshida, T. Kato, K. Sakamoto, T. Murata, A new design of high-resolution small angle X-ray scattering instrument equipped with a multilayer monochromator and a self-rotating anode system, Memoirs Fac. Eng. Tokyo Met. Univ. 44 (1994) 4977–4986.
[18] F. Jahnig, H. Vogel, L. Best, Unifying description of the effect of membrane proteins on lipid order. Verification for the melittin/dimyristoylphosphatidylcholine system, Biochemistry 21 (1982) 6790–6798.
[19] M. Posch, U. Rakusch, C. Mollay, P. Laggner, Cooperative effects in the interaction between melittin and phosphatidylcholine model membranes. Studies by temperature scanning densitometry, J. Biol. Chem. 258 (1983) 1761–1766.
[20] J.F. Nagle, Area/lipid of bilayers from NMR, Biophys. J. 64 (1993) 1476–1481.
[21] K. He, S.J. Ludtke, Y. Wu, H.W. Huang, X-ray scattering with momentum transfer in the plane of membrane. Application to gramicidin organization, Biophys. J. 64 (1993) 157–162.
[22] J.R. Elliott, D. Needham, J.P. Dilger, D.A. Haydon, The effects of bilayer thickness and tension on gramicidin single-channel lifetime, Biochim. Biophys. Acta 735 (1983) 95–103.
[23] M. Cortijo, A. Alonso, J.C. Gomez-Fernandez, D. Chapman, Intrinsic protein–lipid interactions. Infrared spectroscopic studies of gramicidin A, bacteriorhodopsin and Ca^{2+}-ATPase in biomembranes and reconstitution systems, J. Mol. Biol. 157 (1982) 597–618.
[24] D.C. Lee, A.A. Durrani, D. Chapman, A difference infrared spectroscopic studies of gramicidin A, alamethicin and bacteriorhodopsin in perdeuterated dimyristoylphosphatidylcholine, Biochim. Biophys. Acta 769 (1984) 49–56.
[25] V.M. Naik, S. Krimm, Vibrational analysis of the structure of gramicidin A: I. Normal mode analysis, Biophys. J. 49 (1986) 1131–1145.
[26] V.M. Naik, S. Krimm, Vibrational analysis of the structure of gramicidin A: II. Vibrational spectra, Biophys. J. 49 (1986) 1147–1154.
[27] J.N. Israelachvili, Intermolecular and Surface Forces, 2nd edn., Academic Press, New York, 1991, pp. 405–408.
[28] E.J.W. Verwey, J.Th.G. Overbeek, Theory of the stability of lyophobic colloids, in: The Interaction of Sol Particles Having an Electric Double Layer, Elsevier, Amsterdam, 1948, p. 102.
[29] W. Helfrich, Steric interaction of fluid membranes in multilayer systems, Z. Naturforsch. 33 (1978) 305–315.
[30] D. Needham, D.V. Zhelev, The mechanochemistry of lipid vesicles examined by micropipet manipulation techniques, in: M. Rosoff (Ed.), Vesicles, Surfactant Science Series, Vol. 62, Marcel Dekker, New York, 1996, pp. 373–444.